



HAL
open science

Stability in time and consistency between atmospheric corrections: Assessing the reliability of Sentinel-2 products for biodiversity monitoring in tropical forests

Eric Chraibi, Florian de Boissieu, Nicolas Barbier, Sandra Luque,
Jean-Baptiste Féret

► To cite this version:

Eric Chraibi, Florian de Boissieu, Nicolas Barbier, Sandra Luque, Jean-Baptiste Féret. Stability in time and consistency between atmospheric corrections: Assessing the reliability of Sentinel-2 products for biodiversity monitoring in tropical forests. *International Journal of Applied Earth Observation and Geoinformation*, 2022, 112, pp.102884. 10.1016/j.jag.2022.102884 . hal-03747311

HAL Id: hal-03747311

<https://hal.inrae.fr/hal-03747311>

Submitted on 8 Aug 2022

HAL is a multi-disciplinary open access archive for the deposit and dissemination of scientific research documents, whether they are published or not. The documents may come from teaching and research institutions in France or abroad, or from public or private research centers.

L'archive ouverte pluridisciplinaire **HAL**, est destinée au dépôt et à la diffusion de documents scientifiques de niveau recherche, publiés ou non, émanant des établissements d'enseignement et de recherche français ou étrangers, des laboratoires publics ou privés.



Distributed under a Creative Commons Attribution 4.0 International License



Contents lists available at ScienceDirect

International Journal of Applied Earth Observations and Geoinformation

journal homepage: www.elsevier.com/locate/jag

Stability in time and consistency between atmospheric corrections: Assessing the reliability of Sentinel-2 products for biodiversity monitoring in tropical forests

Eric Chraïbi^{a,*}, Florian de Boissieu^{a,b}, Nicolas Barbier^c, Sandra Luque^a, Jean-Baptiste Féret^a^a TETIS (Land, Environment, Remote Sensing and Spatial Information Unit) INRAE, AgroParisTech, Université Montpellier, Montpellier, France^b UMR Eco&Sols, CIRAD, Montpellier, France^c AMAP, Université Montpellier, IRD, CNRS, CIRAD, INRAE, Montpellier, France

ARTICLE INFO

Keywords:

BOA reflectance
MAJA
LaSRC
Overland
Sen2cor
biodivMapR

ABSTRACT

Earth observation satellite imagery is increasingly accessible, and has become a key component for vegetation mapping and monitoring. Sentinel-2 satellites acquire optical images with five days' revisit frequency, which is an important feature to increase the probability of acquisition with reasonable cloud cover in tropical regions. Regular and reliable satellite observations open perspectives for the monitoring of vegetation properties and biodiversity. Atmospheric correction methods (ACMs) producing bottom-of-atmosphere (BOA) reflectance are critical to ensure temporal consistency of higher-level products and optimal sensitivity to changes in vegetation properties. Still their application in tropical regions remains challenging due to complex atmospheric issues. This study aims at performing ACM inter-comparison in the context of tropical forest monitoring. We produced BOA reflectance for a set of Sentinel-2 acquisitions corresponding to a forested area in Cameroon, using four atmospheric correction methods: Sen2cor, MAJA, Overland and LaSRC. We selected five successive acquisitions with moderate to no cloud cover, and computed a set of spectral indices and spectral diversity metrics in order to compare the consistency of these products through time, under the hypothesis that they should remain stable over a short period. We also assessed the agreement between atmospheric correction methods. Two spatial extents were used for the computation of spectral diversity metrics to assess the robustness of the data-driven processes applied to compute spectral diversity. We found that the choice of an ACM did have a significant impact on BOA reflectance and higher-level products. In the visible domain, Overland and LaSRC produced consistent BOA reflectance values, while MAJA and Sen2Cor showed strong variability which could not be explained by changes in surface properties. This directly influenced the temporal consistency of NDVI. Yet, the influence on the temporal consistency for EVI and NDWI was moderate. Spectral diversity metrics were consistent through time for all methods, but to a lesser degree than vegetation indices. When comparing the mean values over the period considered, vegetation indices were stable across methods, but not diversity metrics. Spatial context changes had an impact on the Shannon index, but not on Bray-Curtis dissimilarity. These results suggest that the choice of ACM has major potential implications for tropical forest monitoring.

1. Introduction

1.1. Improving our understanding of the biodiversity crisis with remote sensing

The Biodiversity crisis calls for urgent actions (IPBES, 2019; Turney et al., 2020). The preservation of biodiversity has become a major

challenge for sustainable development from local to global levels. To address these conservation goals, we need operational methods to improve monitoring of ecosystem conditions and to inform conservation planning and support restoration initiatives (Luque et al., 2018). Tropical forests are particularly threatened, facing both direct destruction by human activities and climate change impacts (Barlow et al., 2016; Edwards et al., 2019). In order to coordinate scientific efforts and

* Corresponding author at: Maison de la Télédétection 500 rue Jean-François Breton, 34090 Montpellier, France.

E-mail addresses: eric.chraibi@inrae.fr (E. Chraïbi), florian.deboissieu@inrae.fr (F. de Boissieu), nicolas.barbier@ird.fr (N. Barbier), sandra.luque@inrae.fr (S. Luque), jean-baptiste.feret@inrae.fr (J.-B. Féret).

<https://doi.org/10.1016/j.jag.2022.102884>

Received 29 March 2022; Received in revised form 7 June 2022; Accepted 21 June 2022

Available online 8 July 2022

1569-8432/© 2022 The Authors. Published by Elsevier B.V. This is an open access article under the CC BY license (<http://creativecommons.org/licenses/by/4.0/>).

articulate with decision makers, the Biodiversity Observation Network – which is part of the Group on Earth Observation – focuses on the definition and implementation of Essential Biodiversity Variables (EBVs) (Pereira et al., 2013), designed to harmonize biodiversity monitoring. Global scale retrieval of such variables by the sole means of field surveys is costly and time consuming. Remote sensing has proven to be a strong lead towards the upscaling of biodiversity observation (Skidmore et al., 2015; Pettorelli et al., 2016; Luque et al., 2018; Reddy et al., 2021). Free and open access remote sensing data open up new perspectives for operational biodiversity monitoring over a broad range of ecosystems, providing global coverage, fine spatial resolution, rich spectral information and short revisit period. Original methods taking advantage of these improvements are being developed by the scientific community (Wang and Gamon, 2019). However, operationalization of such methods remains challenging (Portillo-Quintero et al., 2021). We need to ensure that the degree of precision and consistency needed for biodiversity monitoring matches the input remote sensing data.

Sentinel-2 for biodiversity monitoring and caveat regarding atmospheric corrections

The ambitious objective of large-scale remotely sensed biodiversity monitoring seems within reach (Tuomisto et al., 2019; Rocchini et al., 2021; Aguirre-Gutiérrez et al., 2021). Many promising results regarding biodiversity mapping based on the multispectral missions Sentinel-2 and Landsat have been produced (Hošćilo and Lewandowska, 2019; Torresani et al., 2019; Chraïbi et al., 2021). As we aim at reducing the uncertainty in the estimated vegetation properties, the requirements increase in terms of radiometric, spatial and temporal resolutions. Such information includes: i) properties from vegetation cover (Hansen et al., 2013); ii) vegetation function and traits (Houborg et al., 2015; Aguirre-Gutiérrez et al., 2021); iii) biophysical parameters to support species distribution models (Randin et al., 2020). These products could be impacted by uncertainty in surface reflectance measurements acquired by spaceborne sensors.

Atmospheric properties strongly influence top-of-atmosphere (TOA) reflectance measured by optical sensors, due to absorption and scattering from gasses, aerosols and water vapour. These sources of variation of reflectance added to the signal reflected from Earth surface may increase complexity when estimating surface properties, and reduce the consistency of TOA reflectance through time. This is particularly true in tropical regions, where atmospheric corrections are complex due to the high aerosol content and nebulosity (Lonjou et al., 2016; Vermote et al., 2018). Atmospheric correction methods (ACM) aim at accounting for the contribution of aerosol optical thickness (AOT) and water vapour content in the atmosphere, in order to produce bottom-of-atmosphere (BOA) reflectance, which are standard reflectance products processed to estimate surface properties. However, moderate uncertainty on the characterization of AOT, which particularly influences shorter wavelengths in the optical domain, i.e. the visible (VIS) domain, may propagate to uncertainty in the estimated BOA reflectance, and higher-level products, such as spectral indices and biodiversity metrics. Therefore, the characterization of this uncertainty resulting from ACM, from BOA reflectance to higher-level products, appears as a crucial step to ensure the reproducibility and qualification of biodiversity monitoring frameworks.

Comparing atmospheric correction products in the context of thematic studies

The choice of one ACM among many may influence the uncertainty of remote sensing products computed from BOA reflectance. ACM validations are usually based on the comparison between BOA reflectance products and reflectance simulated with radiative transfer models parameterized with ground-based remote sensing aerosol networks (AERONET) (Doxani et al., 2018; Marujo et al., 2021) or field reflectance (Sola et al., 2018). However, these benchmarking exercises do not focus on specific and localized applications. Assessing the temporal consistency of higher-level products obtained from BOA image processing appears relevant when characterizing the potential for

operationalization of specific applications. This criterion may highlight differences between methods that would not be so evident when comparing ACM validation alternatives (Martins et al., 2017; Kuhn et al., 2019). Disregard for the importance of the ACM choice could hamper the reproducibility of the analysis, leading to difficulties for the monitoring of vegetation or even producing flawed results.

The main objective of our study is to substantiate the uncertainty induced by atmospheric correction when using Sentinel-2 data acquired over tropical forests, and to provide guidelines for optical data pre-processing in the context of biodiversity monitoring. Our results will contribute to ensuring the comparability of tropical vegetation studies, and to assessing the reliability of spectral diversity metrics. To achieve this objective, we assessed the temporal stability of Sentinel-2 images and products obtained from four ACMs, and their pairwise agreement over a short period of time. We selected a region in Cameroon as a case study to test different ACM and to compare BOA reflectance, vegetation indices, and spectral diversity metrics over five acquisitions of Sentinel-2.

2. Materials

2.1. Study area

The study area selected as a demonstrator is located in the eastern region of Cameroon, alongside the border with the Central African Republic (Fig. 1). It covers 8400 km² at 14°09E–15°08E and 3°53 N–4°52 N with an average altitude of 642 m. Slopes are present but not too steep: 72% of the image exhibits slopes under 6°. According to the Köppen-Geiger climate classification (Peel et al., 2007) this region is broadly classified as “Am: Tropical savanna climate”. The temperatures are stable throughout the year. The year is divided between a rainy season (March to November) and a dry season (December to February). The vegetation in this region is categorized as closed evergreen lowland forest (Onana, 2015).

2.2. Satellite images

Level-1C images (TOA reflectance) were downloaded from the Copernicus hub (<https://scihub.copernicus.eu/>) for the application of three of the four atmospheric correction algorithms tested here, while Level-2A images (BOA reflectance) corrected with the MAJA processing chain were directly downloaded from the Theia data hub (<https://theia.cnes.fr/>).

Sentinel-2 acquisitions were selected based on visual analysis over the shortest possible time period in order to minimize cloud and haze cover, as well as changes in forest properties. We identified five Sentinel-2 images from tile 33NVE with low cloud cover acquired over a period of less than five weeks in the dry season, between January and February 2018.

3. Methods

3.1. Overview

We identified a set of atmospheric correction methods to assess the stability and agreement of remotely sensed products dedicated to tropical forest functions and biodiversity monitoring. We computed vegetation indices (3.3) and spectral diversity metrics (3.4) from atmospherically corrected images produced from each ACM. We then assessed the temporal stability of reflectance and higher-level metrics for each ACM (4.1). We also measured the agreement between ACM for the computation of vegetation indices and spectral diversity metrics (4.2). Finally, we estimated the influence of the spatial scale of analysis of spectral diversity metrics, as their computation results from data driven analysis and may be sensitive to this factor (4.3). A flowchart providing an overview of the developed methodology to compare

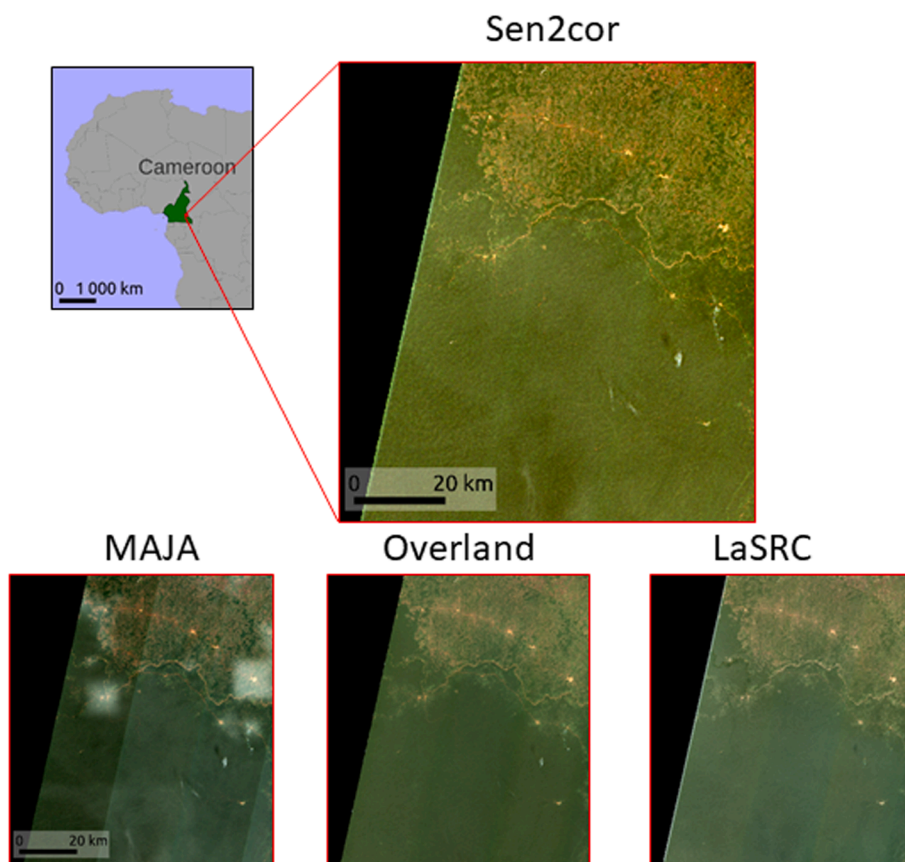


Fig. 1. Tile 33NVE acquired on the 2018/01/01 shown with the four ACM compared in our study.

temporal stability and consistency between ACMs is presented in Fig. 2.

3.2. Atmospheric correction

We selected four ACMS applicable to Sentinel-2 images, three of which (Sen2cor, MAJA, LaSRC) were featured in the Atmospheric Inter-comparison eXercise (ACIX, Doxani, 2018) and are widely used among the remote sensing community.

3.2.1. MAJA

The MACCS-ATCOR Joint Algorithm (MAJA) combines an algorithm for atmospheric correction and cloud screening (MACCS) developed by

CNES, and an atmospheric correction software (ATCOR) developed by DLR (Lonjou et al., 2016). MAJA is based on a multitemporal approach requiring a digital elevation model (DEM) for topographic correction, Ground Image Processing Parameters (GIPP) provided by ESA for each Sentinel-2 tile, and meteorological data when available. The latest version of MAJA includes data from Copernicus Atmosphere Monitoring Service (CAMS) (Rouquié et al., 2017).

3.2.2. Sen2cor

Sen2cor (Main-Knorn et al., 2017) is the atmospheric correction processor developed by Telespazio VEGA Deutschland GmbH on behalf of ESA. It requires the Level-1C product, atmospheric radiative transfer

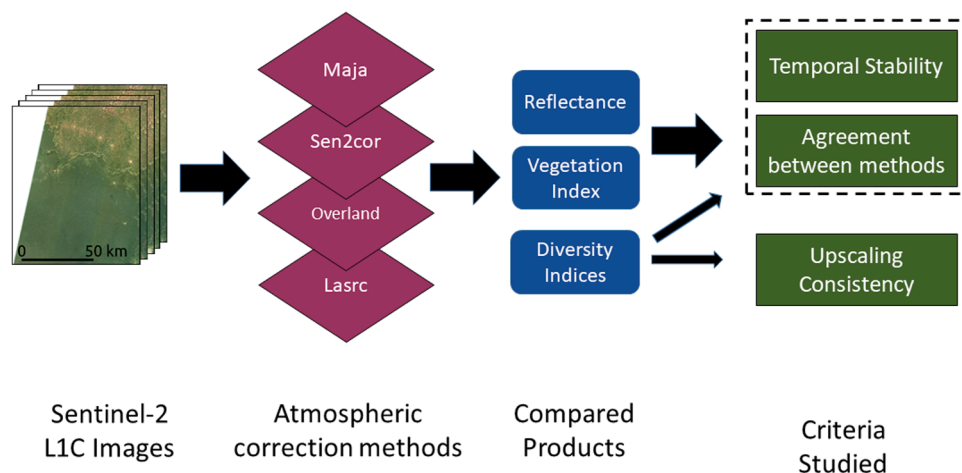


Fig. 2. Flowchart of the developed methodology to compare temporal stability and consistency between ACMs.

look-up tables, and an optional DEM for topographic corrections. Sen2Cor first produces a scene classification, followed by an atmospheric correction based on look-up tables generated by the radiative transfer library LibRadtran (Emde et al., 2016).

3.2.3. Overland

The Overland processor is an optical processing suite developed by Airbus (Poilvé, 2010), which includes algorithms based on the modelling of all parameters contributing to the measured signal constrained by expert knowledge of the region. The physical models SAIL and PROSPECT (Jacquemoud et al., 2009) are used to model the vegetation reflectance, and LOWTRAN-MODTRAN (Kneizys, 1978) is used to model the atmosphere. It also includes topographic correction. Overland was initially developed for the estimation of vegetation biophysical properties, but the inversion of the models allows the retrieval of the top-of-canopy reflectance as a by-product.

3.2.4. LaSRC

The Land Surface Reflectance Code (LaSRC) was originally developed for atmospheric correction of Landsat 8 imagery (Vermote et al., 2016), then extended to Sentinel-2 (Doxani et al., 2018). It is based on the 6S radiative transfer model (Kotchenova and Vermote, 2007) and takes advantage of data from MODIS, MISR and from the National Center for Environmental Prediction Global Data Assimilation System to account for the effects on the atmosphere in the model inversion (Claverie et al., 2018).

3.3. Vegetation index

Vegetation indices are the most common remote sensing products used to monitor vegetation in space and time (Huang et al., 2021). Used as time series (Silva et al., 2013) they allow for the wide scale study of vegetation properties. They are also used as inputs for methods estimating spectral diversity indices, with the purpose of linking them to floristic diversity surveys (He et al., 2009; Rocchini et al., 2017; Wang and Gamon, 2019).

The Normalized Difference Vegetation Index (NDVI) is the normalized difference between reflectance in the near infrared (NIR) and the red band (Eq. (1)). It takes advantage of the contrast in vegetation optical properties between these two spectral domains, with low reflectance of vegetation in the red domain due to the absorption of light by chlorophylls, and the high reflectance in the NIR due to the absence of strong absorbers and multiple scattering related to leaf and canopy structure.

The NDVI tends to saturate when applied to dense vegetation, as is the case in tropical forests (Huete et al., 1997; Van Der Meer et al., 2001). The Enhanced Vegetation Index (EVI) (Huete et al., 1994); Equation (2) was designed to avoid this issue. It was designed for MODIS (Huete et al., 1999) and makes use of coefficients to account for canopy background, and aerosol resistance (Eq. (2)). This index is now also used in Sentinel-2 applications for both temperate (Babcock et al., 2021) and tropical forest situations (Vaglio Laurin et al., 2016). The coefficient values were kept unchanged (Arekhi et al., 2019; Somvanshi and Kumari, 2020).

The Normalized Difference Water Index (NDWI) was designed to measure vegetation water content, by computing the normalized difference between spectral bands in the NIR and shortwave infrared (SWIR) domains (Eq. (3)). Vegetation absorption in the NIR domain is negligible, and increases in the SWIR. This index is also described as less sensitive to atmospheric effects than the NDVI (Gao, 1996).

$$NDVI = \frac{NIR - RED}{NIR + RED} \quad (1)$$

$$EVI = G \times \frac{(NIR - RED)}{(NIR + C1 \times RED - C2 \times BLUE + L)} \quad (2)$$

$$NDWI = \frac{NIRa - SWIR}{NIRa + SWIR} \quad (3)$$

With *BLUE*, *RED*, *NIR*, *NIRa*, *SWIR* the reflectance corresponding to Sentinel-2 spectral bands B2, B4, B8, B8A, B11, respectively; *L* corresponds to the canopy background; *C1* and *C2* are the coefficients of the aerosol resistance term; *G* is the scaling factor. We kept the commonly used values of *L* = 1, *C1* = 6, *C2* = 7.5, and *G* = 2.5.

3.4. Spectral diversity metrics

3.4.1. Diversity indices

Biodiversity as a concept cannot be reduced to a single variable or aspect (DeLong, 1996), but the scientific community has progressively identified indices to study particular aspects of biodiversity. Species diversity can be described using alpha and beta diversity components (Whittaker, 1972). Alpha diversity representing the diversity measured within a sampling unit, and beta diversity highlighting the compositional differences between two sampling units (Magurran, 1988). In the framework of this study, we used the Shannon index as alpha-diversity metric, hereafter named Shannon's *H'*. Shannon's *H'* was quantified as follows (Eq. (4)) (MacArthur, 1965):

$$Shannon's H' = - \sum_{i=1}^N p_i \ln p_i \quad (4)$$

where p_i is the proportion of the i^{th} species among N species inventoried in the sampling unit.

Beta-diversity was computed using Bray-Curtis dissimilarity (BC) (Bray and Curtis, 1957). BC is a commonly used index that quantifies the dissimilarity in species composition between two assemblages weighted by species abundances (Eq. (5)):

$$BC_{UV} = 1 - \frac{2 \sum_{i=1}^N \min(U_i, V_i)}{\sum_{i=1}^N (U_i + V_i)} \quad (5)$$

where for two assemblages U and V , U_i and V_i are the abundances of the species i , and $\min(U_i, V_i)$ is the lowest abundance of the species i , only taking into account species present in both assemblages (Bray and Curtis, 1957; McCarthy and Magurran, 2004). BC ranges between 0 and 1, a value of 0 indicates that two sites are identical, and a value of 1 indicates that they do not share any common species.

3.4.2. Spectral diversity

The effort of the scientific community towards wide-scale biodiversity monitoring has led to the production of several methods aiming at estimating ecological diversity from remotely sensed metrics (Féret and Asner, 2014; Torresani et al., 2019; Laliberté et al., 2020; Marzialetti et al., 2021). Most methods linking spectral reflectance to biodiversity stem from the Spectral Variation Hypothesis (SVH) (Palmer et al., 2002). Féret and Asner (2014) developed a method based on the discretization of the spectral space with an unsupervised clustering algorithm, followed by a cluster inventory to produce diversity indices compatible with taxonomic diversity metrics derived from forest inventories. This method was adapted to Sentinel-2 images, and implemented in the R package *biodivmapR* (Féret and Boissieu, 2020). Our study applied this method to produce spectral diversity metrics from Sentinel-2 images. For each acquisition and for each BOA reflectance product obtained from an ACM, we first applied a filter to remove non-vegetated pixels (NDVI thresholding), shaded pixels (NIR thresholding) and cloudy pixels (Blue thresholding). Then we applied a standardized Principal Components Analysis (PCA) on the spectral information. We performed visual interpretation to select two components enhancing relevant patterns related to vegetation types and discarded components showing noise or sensor artefacts. Finally, we applied k-means clustering on a subset of pixels in order to identify 50 cluster centroids, and associated each pixel

in the image to the nearest cluster centroid.

3.5. Sampling strategy

Our main focus is to study the temporal stability and agreement between ACM for the monitoring of dense tropical forests, and it is based on the hypothesis that dense forest should experience minor changes when analysing the Sentinel-2 acquisitions over less than five weeks, therefore BOA reflectance should show little variations overall. Phenological signal corresponding to leaf fall, leaf flushing, or flowering may influence canopy reflectance, but such effects should be minimal for the time considered, and appear for all ACMs. Local perturbations including forest degradation and logging may also occur, but these should represent a negligible surface when considering large forested extents. The interface between dense forest and other land cover types including bare soil, urban areas and agricultural lands may show strong differences in terms of temporal stability. Pixels including thin clouds, haze or mild atmospheric perturbations and not flagged as cloudy pixels may also lead to reduced temporal consistency and show unpredictable behaviour between methods. Therefore we produced a single mask using the combination of filters applied for each acquisition corrected with each ACM: we applied a NDVI thresholding, selecting only pixels with NDVI higher than 0.4 to discard non-vegetated pixels and low vegetation density areas; a blue thresholding, selecting only pixels with reflectance lower than 7% in the blue domain to discard hazy or cloudy pixels; a NIR thresholding, selecting only pixels with reflectance higher than 15% in the near infrared domain. The application of this mask resulted in an area of about 3 300 km² available for the full tile analysis.

Sentinel-2 acquisitions also show radiometric artefacts corrected when producing Level-1B reflectance data (Baïllarin et al., 2012), which also impact Level-2A (BOA) reflectance data. These artefacts include spectral response non uniformity (SRNU), which is characterised by along-track soft-edged darker or brighter stripes near the detector boundaries (Fig. A1). The data quality is compliant with mission specifications. However, it may correspond to up to 2% reflectance in some cases. SRNU may therefore influence both temporal consistency analysis and ACM inter-comparison. In order to perform an analysis excluding these artefacts, we selected a subset of 225 km² from the Sentinel-2 tile 33NVE, avoiding SNRU identified after visual inspection. This subset was also selected far from clouds, hazy regions, and non-vegetated areas (Fig. 3).

For both the full tile and the subset, the values of reflectance and vegetation indices from all clear pixels were extracted, while spectral diversity indices values were computed from evenly distributed sampling areas corresponding to 100 m radius circular plots. This

specific sampling design was performed in order to ease the comparison between BC dissimilarity matrices. This resulted in 223 areas of interest distant by 800 m in the subset, and 859 distant by 3000 m for the complete tile. The use of these two spatial extents, full tile and subset, also allows for analysis of the stability of spectral diversity metrics when computed over various spatial extents. The computation of these spectral diversity metrics as performed here involves data-driven processing steps (e.g. PCA). Strong differences between a tile subset and a full tile in the contribution to spectral variance may lead to strong differences in terms of spectral species distribution, and corresponding spectral diversity metrics.

3.6. Criteria for inter-comparison

Statistics were produced to assess the consistency of the products obtained for each method, the agreement between the different methods at each date, and the difference between results computed for the subset and the whole tile. We assumed that neither reflectance nor spectral diversity metrics values should change during the period of observation of five weeks. Therefore, we computed the average value over the five acquisitions, for each pixel and each band, spectral index, or spectral diversity metric, and used it as a reference to assess temporal stability. We then computed the linear regression between this mean value and the value for each date. The coefficient of determination (R^2) and the normalised root mean squared error (NRMSE) were used as statistical indicators of the temporal stability for each spectral band, vegetation index, and spectral diversity metric. We computed NRMSE as the RMSE normalised by the interquartile range of the variable in order to ensure comparability of results across variables with different ranges of variation.

The Bray-Curtis dissimilarity was used to measure spectral beta-diversity. A dissimilarity matrix was computed from pairwise comparison of the distribution of spectral species between sampling areas.

4. Results

4.1. Temporal stability of spectral information and related products

4.1.1. Reflectance

The stability of reflectance was assessed through comparison between the values of pixelwise reflectance on each individual image and their mean value over the five acquisitions, for each spectral band and each ACM. Fig. 4 shows the NRMSE (%) and coefficient of determination (R^2) resulting from this comparison. Spectral bands B2 to B5 – Blue, Green, Red and Red-Edge1 – showed the larger differences between ACM

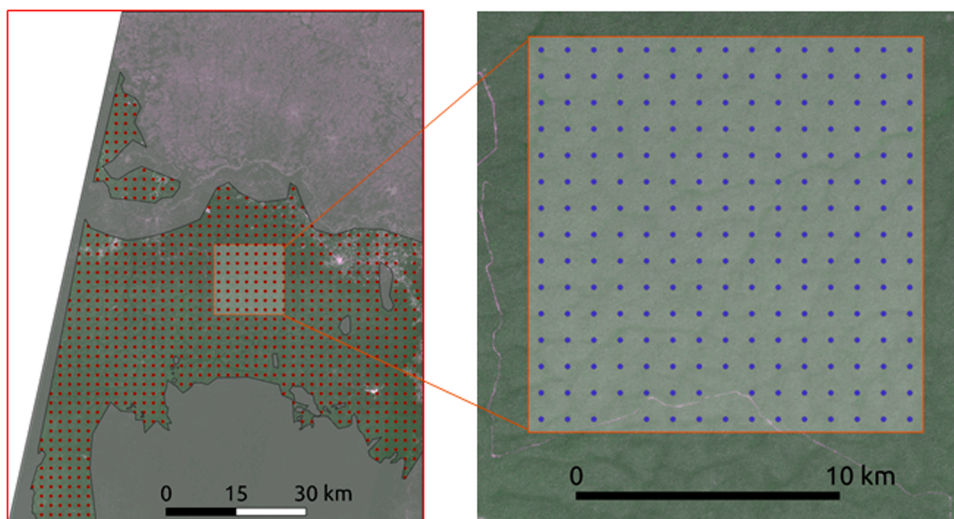


Fig. 3. Sampling strategy applied on the full Sentinel-2 tile after application of a unique mask (left), and on a subset selected to minimize the influence of artefacts and surface changes (right). The greyed out areas represent the mask obtained combining all non vegetated, cloudy or hazy areas observed at any date in the full tile. The square subset encloses the region of interest where no cloud or major artefact are observable during the period of study. This sampling strategy resulted in 859 regularly distributed sampling plots over the whole tile, and 223 inside the subset.

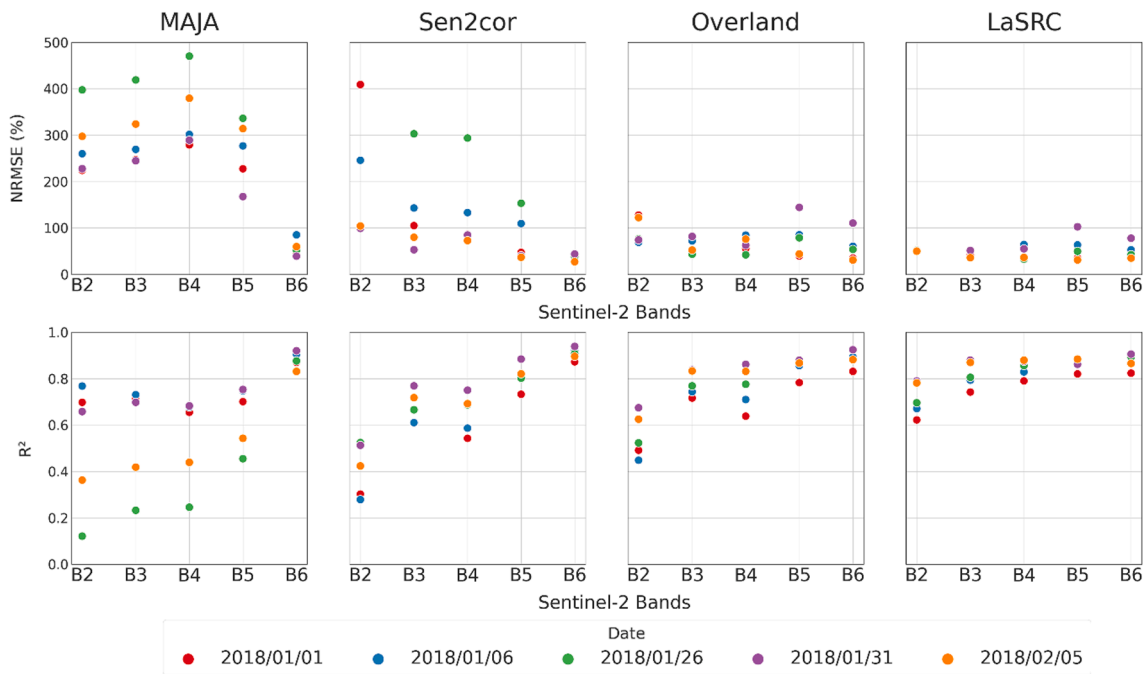


Fig. 4. NRMSE (% of interquartile range) and coefficient of determination computed between reflectance of the total of cloudless vegetated pixels from five individual acquisitions and the average reflectance, for five spectral bands from the VIS (B2, B3, B4) and red edge (B5, B6) domains and each atmospheric correction method over the full tile. (For interpretation of the references to colour in this figure legend, the reader is referred to the web version of this article.)

while for longer wavelengths (Fig. A2), bands B6 to B12, results were similar for all ACM. Among the ACMs, MAJA achieved the lowest temporal consistency in the VIS and Red Edge (RE) domains. The temporal stability corresponding to images produced with Sen2cor was particularly impacted by one acquisition (2018/01/26) which exhibited higher reflectance values in the VIS compared to other acquisitions. LaSRC showed overall better temporal consistency than the other ACMs,

evidenced by lower NRMSE and higher R^2 .

4.1.2. Vegetation indices

The comparison of vegetation indices computed from individual acquisitions with the vegetation indices averaged over all acquisitions only evidenced strong differences in temporal stability between ACM for the NDVI (Fig. 5). For this index, MAJA showed significantly higher

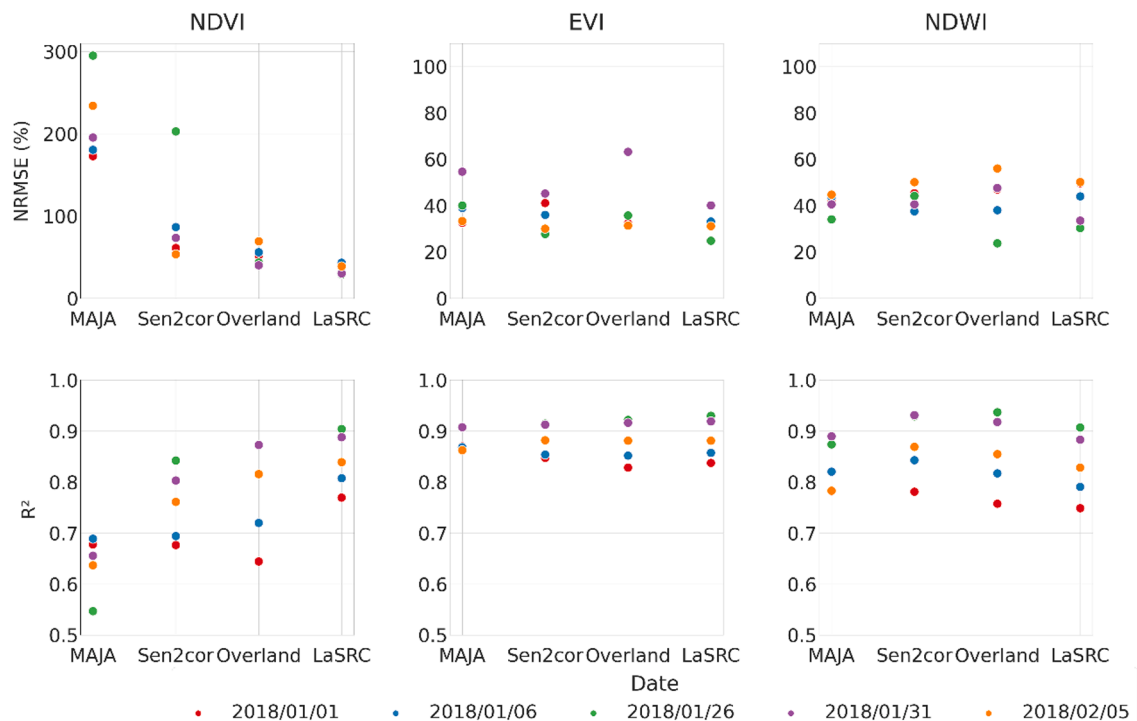


Fig. 5. NRMSE and coefficient of determination of vegetation indices NDVI, EVI and NDWI between individual acquisitions and the corresponding averaged value, for each vegetation index computed over a full Sentinel-2 tile. Different ranges of NRMSE were used to match the ranges of variation.

NRMSE and lower R^2 values than other methods. Sen2Cor showed high NRMSE compared with Overland and LaSRC only for the acquisition from 2018/01/26. EVI and NDWI showed homogenous stability across ACMS.

4.1.3. Spectral diversity metrics

Shannon index

Fig. 6 shows the NRMSE and coefficient of determination between the Shannon's H' obtained from each individual acquisition and the Shannon's H' averaged over the five acquisitions, for the full tile and for a subset of this tile including only dense forest. When considering the subset, the NRMSE ranged between 50% and 100%, with an average value of 61% for all methods. The range of NRMSE was similar over the full tile except for the 2018/01/26 corrected with Sen2Cor, which reached 121%.

Overall, high R^2 values ($R^2 > 0.6$) were obtained between Shannon's H' obtained for each individual acquisition and its averaged value, for all ACM except for the 2018/01/01 corrected with Sen2cor ($R^2 = 0.46$). LaSRC slightly outperformed other methods when comparing stability of computed Shannon's H' through time and consistency for both subset and full tile processing.

Bray-Curtis dissimilarity

Over the subset, values of Bray-Curtis dissimilarities compared with the mean showed similar tendencies for MAJA, Sen2cor and Overland (Fig. 7). For these three methods, R^2 values ranged between 0.59 and 0.85 except for Sen2cor on the 2018/01/01 with a minimum R^2 value of 0.35, while R^2 values obtained from LaSRC systematically exceeded 0.75. Over the full tile, R^2 values decreased significantly and NRMSE increased for all methods except LaSRC.

4.2. Consistency of vegetation and spectral diversity metrics across ACMS

4.2.1. Vegetation indices

NDVI

The mean value of NDVI over the five acquisitions was computed for each ACM (Fig. 8). The pairwise comparison of this mean NDVI over the subset showed high consistency between methods, with a high coefficient of determination ($R^2_{min} = 0.87$). Coefficients of determination were overall lower when comparing the NDVI values over the full tile.

The lowest value ($R^2 = 0.36$) was obtained between MAJA and LaSRC even though the same combination of methods produces amongst the highest values for the coefficient of determination over the subset ($R^2 = 0.97$). Both EVI and NDWI reached high values of correlations across methods at full tile scale ($R^2 > 0.90$; Fig A5, A6).

4.2.2. Spectral diversity metrics

Shannon Index

Pairwise comparison of the mean Shannon index between ACMS resulted in moderate to strong correlation for both subset and full tile analysis, with R^2 ranging from 0.50 to 0.82 (Fig. 9). The coefficients of determination were consistently higher for the full tile analysis than for the subset analysis.

Bray-Curtis dissimilarity

The mean values of Bray-Curtis dissimilarities over the subset reached moderate to high correlation between ACM ($0.43 < R^2 < 0.81$). R^2 values decreased and NRMSE values increased for all pairs of ACMS compared over the full tile ($0.19 < R^2 < 0.54$), except for the Overland-Sen2cor pair for which the results remained stable (Fig. 10).

4.3. Impact of the upscaling of the study area on spectral diversity metrics

4.3.1. Shannon index

The coefficient of determination obtained when comparing the Shannon's H' computed from the subset and from the full tile was computed for each method at each date in order to assess the consistency of the diversity indices produced from different spatial extents (Table A7). This property is key to ensure scalability of diversity mapping. LaSRC consistently achieved the highest R^2 values at around 0.50 for all dates, and other methods punctually reached R^2 values around 0.30. Results for all methods were considerably improved when comparing the mean Shannon's H' over the whole period.

4.3.2. Bray-Curtis dissimilarity

Bray-Curtis dissimilarity values compared between the subset and full tile were consistent ($0.51 < R^2 < 0.98$) for all ACMS except one image produced with Sen2cor ($R^2 = 0.09$ on the 2018/01/01; Table 1). LaSRC exhibited values of R^2 statistic over 0.90 for all acquisitions. MAJA and Overland punctually showed lower values, with $R^2 = 0.53$ for

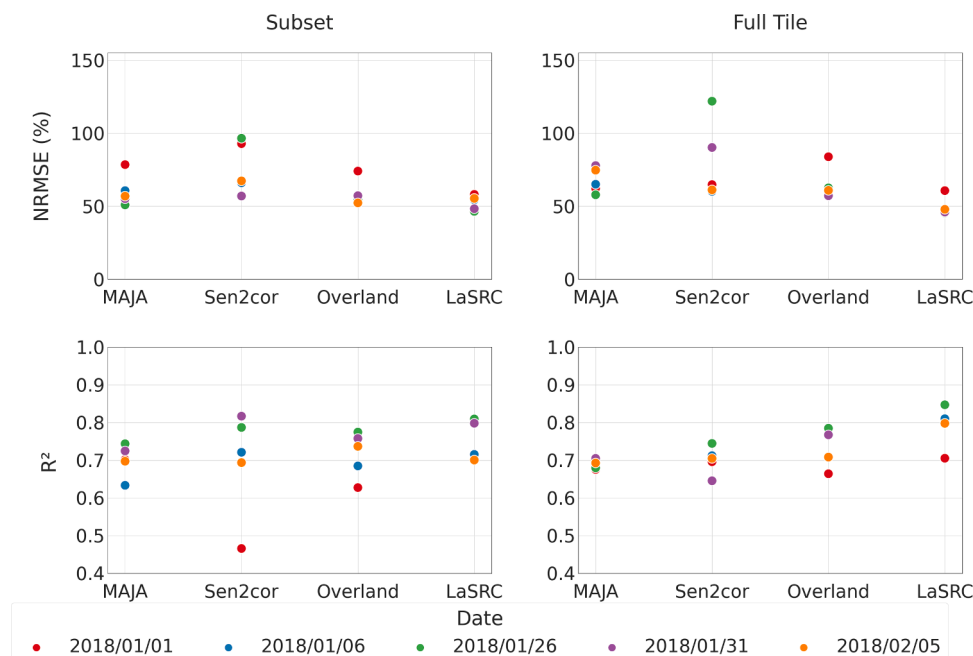


Fig. 6. NRMSE and coefficient of determination between Shannon's H' on five individual acquisitions and the corresponding average over the full tile.

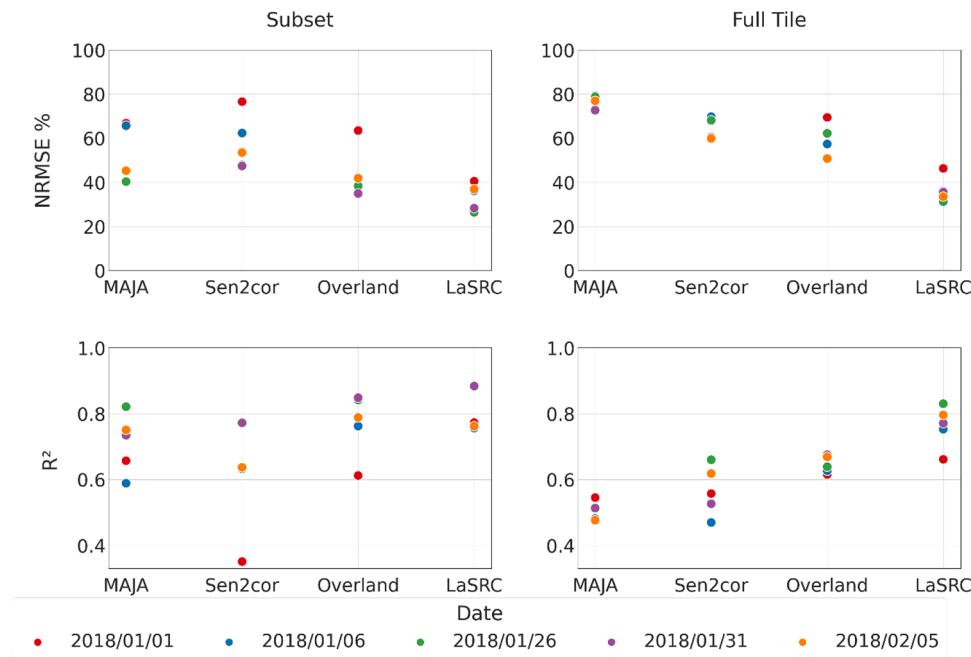


Fig. 7. NRMSE and coefficient of determination between Bray-Curtis Dissimilarities on five individual acquisitions and the corresponding average over the full tile.

MAJA on the 2018/02/05, and $R^2 = 0.58$ for Overland on the 2018/01/01.

4.4. Overall comparison of performances

The capacity of ACMs to produce BOA reflectance, spectral indices and spectral diversity metrics showing temporal stability, and their capacity to produce consistent spectral diversity metrics when using different spatial extents of analysis for individual acquisitions is summarized in Table 2. These results highlight that LaSRC outperforms other methods based on the criteria of our inter-comparison, showing good overall performances in most situations. They also show the reliability of three products for all atmospheric correction methods: BOA reflectance for B6 to B12, EVI and NDWI.

5. Discussion

5.1. Temporal stability

The TOA reflectance is increasingly influenced by atmospheric properties when moving towards shorter wavelengths in the VIS due to the increasing scattering. This makes atmospheric corrections more complex in the VIS, particularly in the context of forested ecosystems in the tropics, because of the presence of haze and bioaerosols (Martins et al., 2017). Here, ACM inter-comparison showed that all ACM produced consistent Sentinel-2 reflectance in time for the infrared domain (Table 3). Sen2cor and MAJA showed strong temporal variability of reflectance in the VIS and first part of the RE domain. This contrasts with the results reported from other studies for these methods over other landscapes (Sola et al., 2018), and confirms the good performance of LaSRC when compared with 6S radiative transfer and AERONET measurements (Doxani et al., 2018; Marujo et al., 2021). The reflectance measured in the VIS is crucial for the monitoring of multiple properties of vegetation (Horler et al., 1983) and has been linked to taxonomic Beta diversity (Polley et al., 2019).

Vegetation indices are commonly regarded as less sensitive to artefacts than the reflectance values. We evidenced strong variations in NDVI at pixel scale over a short period of time for MAJA, and identified one acquisition when the NDVI computed from Sen2cor data

significantly differed from the other acquisitions. This supports results from Moravec et al. (2021) who evidenced the influence of ACM on NDVI. In comparison, EVI, NDWI and Shannon's H' values showed consistent behaviour over time. Bray-Curtis dissimilarity only remained stable in time when applied to LaSRC corrected images, pointing at the importance of the reflectance stability for spectral diversity metrics.

While the results could suggest the use of one method over the other, it cannot conclude definitively on the quality of the considered ACMs without validation from field data. The chosen criteria of time stability of vegetation and diversity indices may also favour methods with stable but incorrect results in the considered time period. Further studies considering the stability of ACMs are recommended, with criteria relevant to each considered field of application. Moreover, change detection and monitoring are regular goals of environmental studies. An over-smoothing caused by the ACM would not be adapted for that kind of applications. Therefore, a comparison of ACMs stability with field validations from case studies in different conditions are needed to provide support on the ACM choice. Finally, the correction of directional reflectance (Roy et al. 2016) could further improve results by reducing artefacts that are particularly strong in the VIS (Flood, 2020) and close to the equator (Franch et al., 2019). However, such corrections are not yet widespread and standardized among related ecological studies.

5.2. Agreement between methods

The EVI remained stable across methods when comparing individual acquisitions (Fig. A4), while poor agreement was observed for the NDVI and NDWI (Fig. 7, Fig. A3). However, the agreement between methods was significantly improved when averaging spectral indices over the five acquisitions. The production of time series syntheses, such as monthly cloud-free syntheses may then contribute to reducing artefacts in cloudy regions (Fig. A5, Fig. A6). However, this may prevent from detecting subtle changes in vegetation properties induced, for example, by phenology (Misra et al., 2020).

Atmospheric corrections were particularly challenging for two acquisitions. The acquisition from 2018/01/26 (MAJA and Sen2cor), and the acquisition from 2018/02/05 (MAJA). No major clouds were left in the masked image, but their presence may have caused an offset in reflectance values overall, which greatly decreased correlation relations,

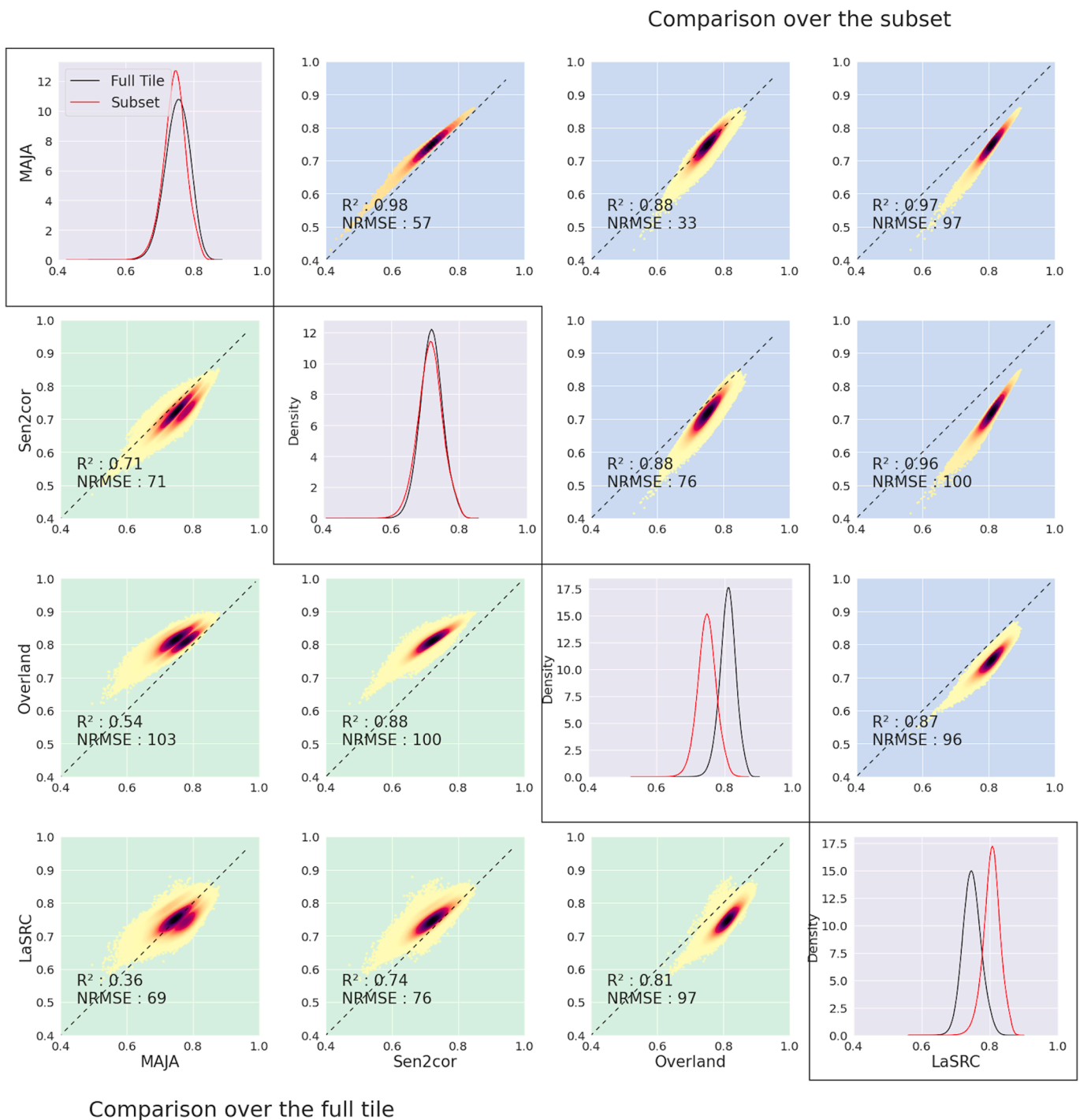


Fig. 8. Comparison of Mean NDVI values between ACMs. The diagonal shows the distribution of mean NDVI values for each ACM, the lower left shows the density plots when comparing pairs of ACMs over the full tile, and the upper right the density plots between ACMs when comparing over the subset.

and increased the measured error. This could have major implications in the use of partially masked images, as even slight atmospheric perturbations induced by haze that leave little to no visual evidence can impact the reflectance values for seemingly cloud free pixels.

Shannon index consistency between methods was improved when comparing subset with full tile results (Fig. 9), as it contained a wider range of Shannon values, and the method used was able to effectively differentiate low and high diversity regions, but less so to distinguish small variations between regions of high diversity. The improvement of results can therefore be understood as statistical by-product of the increased spectral heterogeneity. BC results showed the opposite

tendency: with a reduced heterogeneity in a considered area, the dissimilarity between two sites in this area was more consistent across ACM.

5.3. Impact of the upscaling of the study area over spectral diversity metrics

Working on the average value of spectral diversity over a limited set of (close to) successive Sentinel-2 acquisitions did ensure high stability of the spectral diversity metrics with different spatial contexts, particularly for Shannon's H' (Table 1). The PCA applied to Sentinel-2 image is

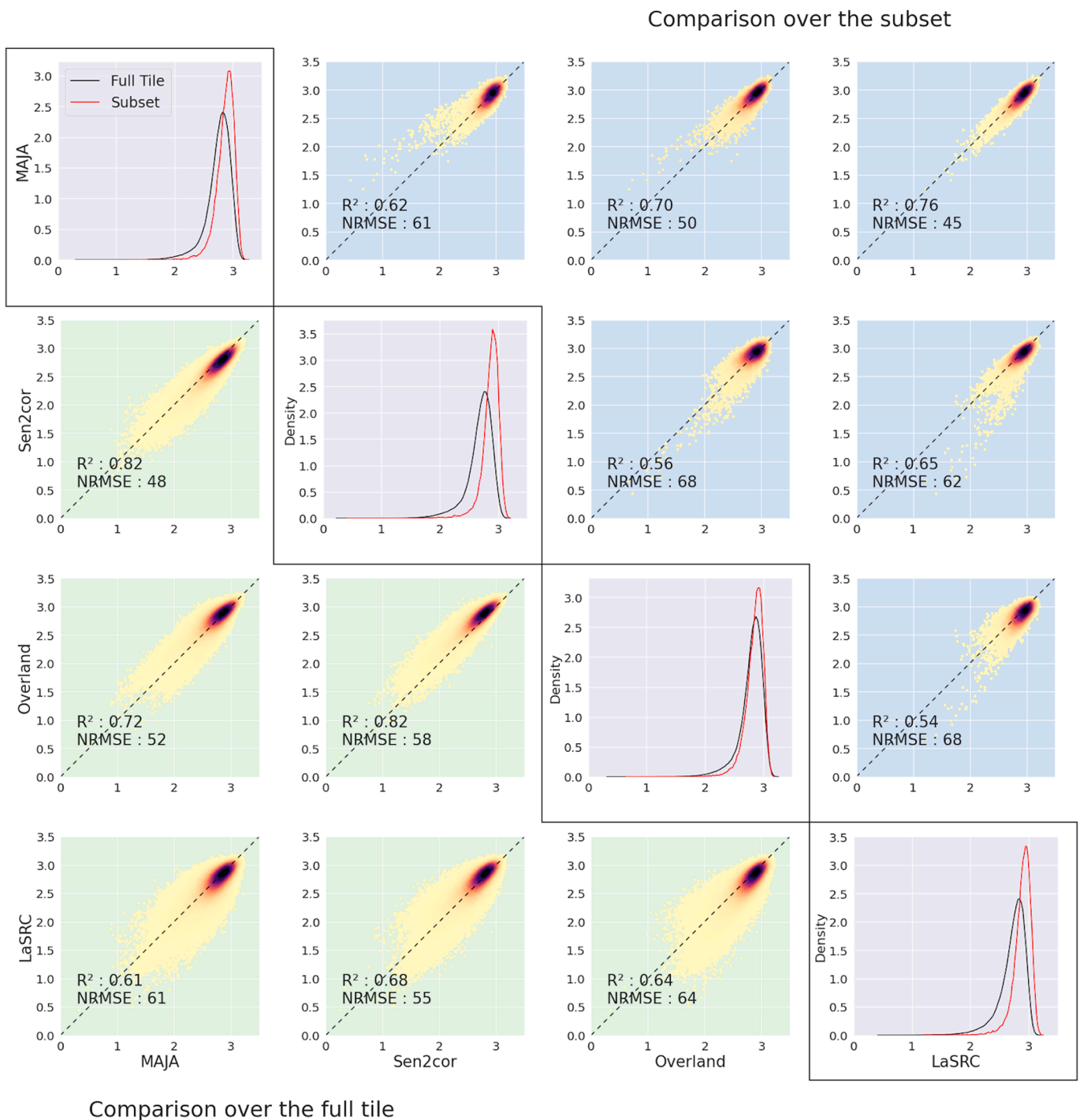


Fig. 9. Comparison of mean Shannon index produced with biodivMapR between ACM. The diagonal shows the distribution of mean Shannon index values for each ACM for the subset and the full tile. The lower left shows the density plots when comparing pairs of ACMs over the full tile, and the upper right the density plots between ACMs when comparing over the subset.

a data driven process. In this study, we prioritised reproducibility, therefore we chose only two components for each ACM at each date. Hence, disparities in components could have a large impact on the spectral diversity metrics obtained. Principal components may change from one Sentinel-2 acquisition to another covering the same spatial extent, as well as their selection based on visual analysis, with possible negative impact on the temporal consistency of spectral diversity metrics over short periods of time. PCA was used in this study as it is commonly used for spectral diversity metrics computation (Féret, 2014; Dahlin, 2016; Onyia et al., 2019; Laliberté et al., 2020). However other

dimensionality reduction methods could be considered (Gholizadeh et al., 2018; Hauser et al., 2021; Jia et al., 2022), in combination with a standardized procedure for feature selection. The tasselled cap transform (Shi and Xu, 2019) could potentially solve both the issue of dimensionality reduction and feature selection, as it produces three physically meaningful bands for which no subsequent selection would be needed.

The results of this study show both the reliability of vegetation indices, and the possibility to keep improving spectral diversity metrics to ensure robust biodiversity monitoring from available remote sensing

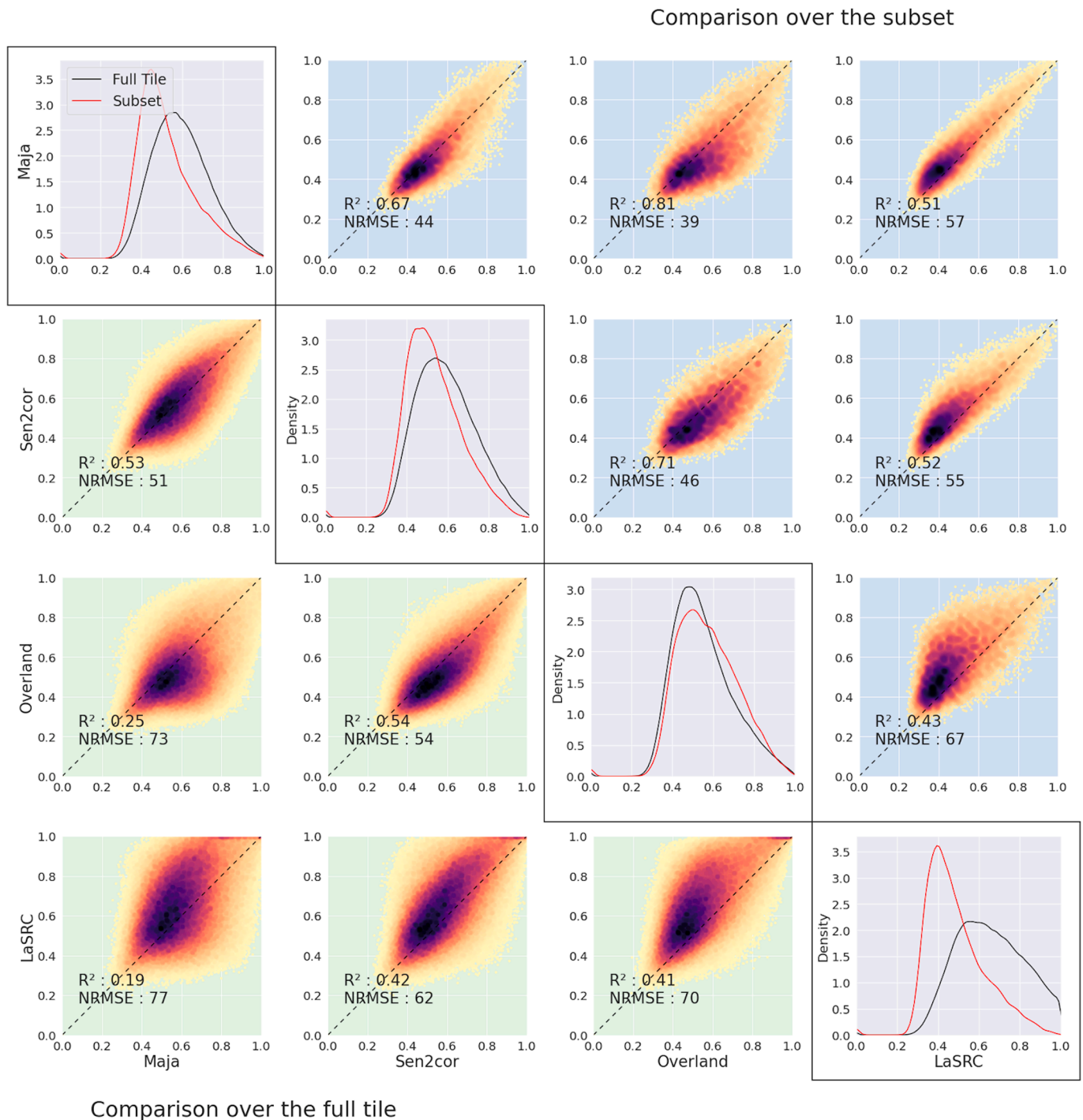


Fig. 10. Comparison of mean Bray-Curtis produced with biodivMapR between ACM. The diagonal shows the distribution of mean Bray-Curtis values for each ACM for the subset and the full tile. The lower left shows the density plots when comparing pairs of ACMs over the full tile, and the upper right the density scatterplots between ACMs when comparing over the subset.

Table 1

Coefficient of determination for Bray-Curtis dissimilarities computed between the subset and the full tile. Values in bold correspond to the highest value of R² for a given date.

	2018/ 01/01	2018/ 01/06	2018/ 01/26	2018/ 01/31	2018/ 02/05	Average
MAJA	0.72	0.98	0.81	0.75	0.53	0.92
Sen2Cor	0.09	0.62	0.55	0.91	0.51	0.78
Overland	0.58	0.72	0.98	0.74	0.81	0.93
LaSRC	0.98	0.91	0.96	0.97	0.97	0.99

data. Thus, one possible way of improving diversity metrics could be to use vegetation indices as input for the calculation of spectral diversity, instead of using reflectance which may show lower temporal consistency depending on the ACM selected to produce BOA reflectance that is less reliable.

6. Conclusion

The application of the four different ACM resulted in contrasted temporal stability of the reflectance, in particular for the visible domain

Table 2

Synthesis of results for temporal Stability and Upscaling Consistency. Green checkmarks indicate good overall performance (indicated by all coefficient of determination values above 0.7), yellow checkmarks indicate moderate performances to good performances (at least one coefficient of determination between 0.3 and 0.7) and red checkmarks indicate poor to moderate performances (at least one coefficient of determination under 0.3).

	Temporal Stability						Tile vs. subset		
	BOA reflectance (S2 bands)		Vegetation indices			Spectral diversity		Spectral diversity	
	B2- B5	B6-B12	NDVI	EVI	NDWI	Alpha	Beta	Alpha	Beta
MAJA									
Sen2cor									
Overland									
LaSRC									

and part of the red edge domain (400–710 nm). While MAJA and Sen2Cor showed strong temporal variability on this spectral domain, Overland and LaSRC presented significantly higher stability. These variations could explain the differences in the stability of spectral indices. NDVI computed from MAJA and Sen2cor BOA was less consistent than LaSRC and Overland. NDWI and EVI were stable for all methods.

When using the mean value over the whole period, NDWI showed very high consistency across all methods for both the subset and the full tile. NDVI presented a slightly lower degree of consistency, with only one pair of methods with differing results over the full tile (MAJA-LaSRC). The value of Shannon's H' was relatively comparable between ACMs when processing either the full Sentinel-2 tile or a subset. The value of the Bray-Curtis dissimilarity showed lower consistency between methods. For all methods and indices, the computation of a mean value from successive acquisitions resulted in improved consistency between ACMs. The spatial extent encompassed to compute spectral diversity metrics showed strong influence on the Shannon's H' . This was observed to a lesser extent for Bray-Curtis dissimilarity, except for images corrected with LaSRC, which showed consistent dissimilarity when computed either from a full tile or from an image subset.

Our results highlight the importance of ACM in the context of tropical forest monitoring, even for the computation of NDVI, which is certainly the most popular Sentinel-2 product. On the other hand, we also showed that wisely selected spectral indices should be suitable for forest monitoring despite the strong inconsistency of BOA reflectance in the VIS obtained for some of the ACMs studied here: even if EVI uses reflectance from VIS spectral bands, in particular the band B2, it showed higher consistency through time than NDVI. Finally, higher-level spectral diversity products aiming at providing information on alpha and beta components of forest biodiversity showed contrasted consistency through time between ACM. LaSRC appeared as the most suitable ACM for the computation of spectral diversity metrics in tropical forests. Further investigations are now needed to validate these results with additional in situ information.

Declaration of Competing Interest

The authors declare that they have no known competing financial interests or personal relationships that could have appeared to influence the work reported in this paper.

Acknowledgements

This research was supported by the Agence Nationale de la Recherche (France) (BioCOP project—ANR-17-CE32-0001) and the TOSCA program grant of the French Space Agency (CNES) (HyperTropik/HyperBIO project). The authors thank the Centre National d'Etudes Spatiales and the THEIA data and service center for distributing L2A

Sentinel-2 products produced with MAJA. The authors thank the European Space Agency for providing free and open access to Sen2Cor. The authors thank the developers of LaSRC. The authors thank Hervé Poilve and Airbus for allowing using Overland for this study.

Appendix A. Supplementary material

Supplementary data to this article can be found online at <https://doi.org/10.1016/j.jag.2022.102884>.

References

- Aguirre-Gutiérrez, J., Rifai, S., Shenkin, A., Oliveras, I., Bentley, L.P., Svátek, M., Girardin, C.A.J., Both, S., Riutta, T., Berenguer, E., Kissling, W.D., Bauman, D., Raab, N., Moore, S., Farfan-Rios, W., Figueiredo, A.E.S., Reis, S.M., Ndong, J.E., Ondo, F.E., N'ssi Bengone, N., Mihindou, V., Moraes de Seixas, M.M., Adu-Bredu, S., Abernethy, K., Asner, G.P., Barlow, J., Burslem, D.F.R.P., Coomes, D.A., Cernusak, L.A., Dargie, G.C., Enquist, B.J., Ewers, R.M., Ferreira, J., Jeffery, K.J., Joly, C.A., Lewis, S.L., Marimon-Junior, B.H., Martin, R.E., Morandi, P.S., Phillips, O.L., Quesada, C.A., Salinas, N., Schwantes Marimon, B., Silman, M., Teh, Y.A., White, L.J., Malhi, Y., 2021. Pantropical modelling of canopy functional traits using Sentinel-2 remote sensing data. *Remote Sens. Environ.* 252, 112122. <https://doi.org/10.1016/j.rse.2020.112122>.
- Arekhi, M., Goksel, C., Balik Sanli, F., Senel, G., 2019. Comparative evaluation of the spectral and spatial consistency of sentinel-2 and Landsat-8 OLI data for ignea longa forest. *IJGI* 8, 56. <https://doi.org/10.3390/ijgi8020056>.
- Babcock, C., Finley, A.O., Looker, N., 2021. A Bayesian model to estimate land surface phenology parameters with harmonized Landsat 8 and Sentinel-2 images. *Remote Sens. Environ.* 261, 112471. <https://doi.org/10.1016/j.rse.2021.112471>.
- Baillarin, S.J., Meygret, A., Dechoz, C., Petrucci, B., Lacherade, S., Tremas, T., Isola, C., Martimort, P., Spoto, F., 2012. SENTINEL-2 LEVEL 1 PRODUCTS AND IMAGE PROCESSING PERFORMANCES, in: Shortis, M and ElSheimy, N (Ed.), XXII ISPRS CONGRESS, TECHNICAL COMMISSION I, International Archives of the Photogrammetry, Remote Sensing and Spatial Information Sciences. Int Soc Photogrammetry & Remote Sensing; Hexagon; ESRI; RMIT Univ, Sch Math Geospatial Sci, pp. 197–202.
- Barlow, J., Lennox, G.D., Ferreira, J., Berenguer, E., Lees, A.C., Nally, R.M., Thomson, J. R., Ferraz, S.F.d.B., Louzada, J., Oliveira, V.H.F., Parry, L., Ribeiro de Castro Solar, R., Vieira, I.C.G., Aragão, L.E.O.C., Begotti, R.A., Braga, R.F., Cardoso, T.M., de Oliveira, R.C., Souza Jr, C.M., Moura, N.G., Nunes, S.S., Siqueira, J.V., Pardini, R., Silveira, J.M., Vaz-de-Mello, F.Z., Veiga, R.C.S., Venturieri, A., Gardner, T.A., 2016. Anthropogenic disturbance in tropical forests can double biodiversity loss from deforestation. *Nature* 535 (7610), 144–147. <https://doi.org/10.1038/nature18326>.
- Bray, J.R., Curtis, J.T., 1957. An ordination of the upland forest communities of Southern Wisconsin. *Ecol. Monogr.* 27 (4), 325–349. <https://doi.org/10.2307/1942268>.
- Chraïbi, E., Arnold, H., Luque, S., Deacon, A., Magurran, A., Féret, J.-B., 2021. A remote sensing approach to understanding patterns of secondary succession in tropical forest. *Remote Sensing* 13, 2148. <https://doi.org/10.3390/rs13112148>.
- Claverie, M., Ju, J., Masek, J.G., Dungan, J.L., Vermote, E.F., Roger, J.-C., Skakun, S.V., Justice, C., 2018. The harmonized landsat and Sentinel-2 surface reflectance data set. *Remote Sens. Environ.* 219, 145–161. <https://doi.org/10.1016/j.rse.2018.09.002>.
- Dahlin, K.M., 2016. Spectral diversity area relationships for assessing biodiversity in a wildland-agriculture matrix. *Ecol Appl* 26, 2758–2768. <https://doi.org/10.1002/eap.1390>.
- Doxani, G., Vermote, E., Roger, J.-C., Gascon, F., Adriaensen, S., Frantz, D., Hagolle, O., Hollstein, A., Kirches, G., Li, F., Louis, J., Mangin, A., Pahlevan, N., Pflug, B., Vanhellemont, Q., 2018. Atmospheric correction inter-comparison exercise. *Remote Sens.* 10 (3), 352. <https://doi.org/10.3390/rs10020352>.

- Edwards, D.P., Socolar, J.B., Mills, S.C., Burivalova, Z., Koh, L.P., Wilcove, D.S., 2019. Conservation of tropical forests in the anthropocene. *Curr. Biol.* 29 (19), R1008–R1020. <https://doi.org/10.1016/j.cub.2019.08.026>.
- Emde, C., Buras-Schnell, R., Kylling, A., Mayer, B., Gasteiger, J., Hamann, U., Kylling, J., Richter, B., Pause, C., Dowling, T., Bugliaro, L., 2016. The libRadtran software package for radiative transfer calculations (version 2.0.1). *Geosci. Model Dev.* 9 (5), 1647–1672. <https://doi.org/10.5194/gmd-9-1647-2016>. <https://doi.org/10.5194/gmd-9-1647-2016-supplement>.
- Féret, J., Boissieu, F., 2020. biodivMAPr: An r package for α - and β -diversity mapping using remotely sensed images. *Methods Ecol Evol* 11, 64–70. <https://doi.org/10.1111/2041-210X.13310>.
- Féret, J.-B., Asner, G.P., 2014. Mapping tropical forest canopy diversity using high-fidelity imaging spectroscopy. *Ecol Appl* 24 (6), 1289–1296.
- Flood, N., 2020. Assessing BRDF effects in the Sentinel-2 Level 2A product in the Australian landscape 1391404 Bytes. <https://doi.org/10.6084/M9.FIGSHARE.12820268.V1>.
- Franch, B., Vermote, E., Skakun, S., Roger, J.-C., Masek, J., Ju, J., Villaescusa-Nadal, J., Santamaria-Artigas, A., 2019. A method for Landsat and Sentinel 2 (HLS) BRDF normalization. *Remote Sensing* 11, 632. <https://doi.org/10.3390/rs11060632>.
- Gao, B.-C., 1996. NDWI—a normalized difference water index for remote sensing of vegetation liquid water from space. *Remote Sens. Environ.* 58 (3), 257–266.
- Gholizadeh, H., Gamon, J.A., Zyguelbaum, A.I., Wang, R., Schweiger, A.K., Cavender-Bares, J., 2018. Remote sensing of biodiversity: Soil correction and data dimension reduction methods improve assessment of α -diversity (species richness) in prairie ecosystems. *Remote Sens. Environ.* 206, 240–253. <https://doi.org/10.1016/j.rse.2017.12.014>.
- Hansen, M.C., Potapov, P.V., Moore, R., Hancher, M., Turubanova, S.A., Tyukavina, A., Thau, D., Stehman, S.V., Goetz, S.J., Loveland, T.R., Kommareddy, A., Egorov, A., Chini, L., Justice, C.O., Townshend, J.R.G., 2013. High-resolution global maps of 21st-century forest cover change. *Science* 342 (6160), 850–853.
- Hausler, L.T., Timmermans, J., van der Windt, N., Sil, Á.F., César de Sá, N., Soudzilovskaia, N.A., van Bodegom, P.M., 2021. Explaining discrepancies between spectral and in-situ plant diversity in multispectral satellite earth observation. *Remote Sens. Environ.* 265, 112684. <https://doi.org/10.1016/j.rse.2021.112684>.
- He, K.S., Zhang, J., Zhang, Q., 2009. Linking variability in species composition and MODIS NDVI based on beta diversity measurements. *Acta Oecologica* 35 (1), 14–21. <https://doi.org/10.1016/j.actao.2008.07.006>.
- Horler, D.N.H., Dockray, M., Barber, J., 1983. The red edge of plant leaf reflectance. *Int. J. Remote Sens.* 4 (2), 273–288. <https://doi.org/10.1080/01431168308948546>.
- Hościo, A., Lewandowska, A., 2019. Mapping Forest Type and Tree Species on a Regional Scale Using Multi-Temporal Sentinel-2 Data. *Remote Sensing* 11, 929. <https://doi.org/10.3390/rs11080929>.
- Houborg, R., Fisher, J.B., Skidmore, A.K., 2015. Advances in remote sensing of vegetation function and traits. *Int. J. Appl. Earth Obs. Geoinf.* 43, 1–6. <https://doi.org/10.1016/j.jag.2015.06.001>.
- Huang, S., Tang, L., Hupy, J.P., Wang, Y., Shao, G., 2021. A commentary review on the use of normalized difference vegetation index (NDVI) in the era of popular remote sensing. *J. For. Res.* 32 (1), 1–6. <https://doi.org/10.1007/s11676-020-01155-1>.
- Huete, A., Justice, C., Liu, H., 1994. Development of vegetation and soil indices for MODIS-EOS. *Remote Sens. Environ.* 49 (3), 224–234. [https://doi.org/10.1016/0034-4257\(94\)90018-3](https://doi.org/10.1016/0034-4257(94)90018-3).
- Huete, A.R., HuiQing Liu, van Leeuwen, W.J.D., 1997. The use of vegetation indices in forested regions: issues of linearity and saturation, in: IGARSS'97. 1997 IEEE International Geoscience and Remote Sensing Symposium Proceedings. Remote Sensing - A Scientific Vision for Sustainable Development. Presented at the IGARSS'97. 1997 IEEE International Geoscience and Remote Sensing Symposium Proceedings. Remote Sensing - A Scientific Vision for Sustainable Development, IEEE, Singapore, pp. 1966–1968. <https://doi.org/10.1109/IGARSS.1997.609169>.
- Huete, A., Justice, C., Van Leeuwen, W., 1999. MODIS vegetation index (MOD13). Algorithm theoretical basis document 3.
- IPBES, 2019. Global assessment report on biodiversity and ecosystem services of the Intergovernmental Science-Policy Platform on Biodiversity and Ecosystem Services. E. S. Brondizio, J. Settele, S. Díaz, and H. T. Ngo (editors). IPBES secretariat, Bonn, Germany. 1148 pages. <https://doi.org/10.5281/zenodo.3831673>.
- Jacquemois, S., Verhoef, W., Baret, F., Bacour, C., Zarco-Tejada, P.J., Asner, G.P., François, C., Ustin, S.L., 2009. PROSPECT+SAIL models: A review of use for vegetation characterization. *Remote Sens. Environ.* 113, S56–S66. <https://doi.org/10.1016/j.rse.2008.01.026>.
- Jia, W., Sun, M., Lian, J., Hou, S., 2022. Feature dimensionality reduction: a review. *Complex Intell. Syst.* 8 (3), 2663–2693. <https://doi.org/10.1007/s40747-021-00637-x>.
- Kneizys, F.X., 1978. Atmospheric Transmittance And Radiance: The Lowtran Code, in: Sepucha, R. (Ed.), . Presented at the 1978 Technical Symposium East, Washington, D.C., pp. 6–8. <https://doi.org/10.1117/12.956522>.
- Kotchenova, S.Y., Vermote, E.F., 2007. Validation of a vector version of the 6S radiative transfer code for atmospheric correction of satellite data Part II Homogeneous Lambertian and anisotropic surfaces. *Appl. Opt.* 46 (20), 4455. <https://doi.org/10.1364/AO.46.004455>.
- Kuhn, C., de Matos Valerio, A., Ward, N., Loken, L., Sawakuchi, H.O., Kampel, M., Richey, J., Stadler, P., Crawford, J., Striegl, R., Vermote, E., Pahlevan, N., Butman, D., 2019. Performance of Landsat-8 and Sentinel-2 surface reflectance products for river remote sensing retrievals of chlorophyll-a and turbidity. *Remote Sens. Environ.* 224, 104–118. <https://doi.org/10.1016/j.rse.2019.01.023>.
- Laliberté, E., Schweiger, A.K., Legendre, P., He, F., 2020. Partitioning plant spectral diversity into alpha and beta components. *Ecol Lett* 23 (2), 370–380. <https://doi.org/10.1111/ele.13429>.
- Lonjou, V., Desjardins, C., Hagolle, O., Petrucci, B., Tremas, T., Dejus, M., Makarau, A., Auer, S., 2016. MACCS-ATCOR joint algorithm (MAJA). In: Comerón, A., Kassianov, E.I., Schäfer, K. (Eds.), Presented at the SPIE Remote Sensing. United Kingdom, Edinburgh, p. 1000107. <https://doi.org/10.1117/12.2240935>.
- Luque, S., Pettorelli, N., Vihervaara, P., Wegmann, M., Vamosi, J., 2018. Improving biodiversity monitoring using satellite remote sensing to provide solutions towards the 2020 conservation targets. *Methods Ecol. Evol.* 9 (8), 1784–1786. <https://doi.org/10.1111/2041-210X.13057>.
- MacArthur, R.H., 1965. Patterns of species diversity. *Biol. Rev.* 40 (4), 510–533. <https://doi.org/10.1111/j.1469-185X.1965.tb00815.x>.
- Magurran, A.E. (Ed.), 1988. *Ecological Diversity and Its Measurement*. Springer Netherlands, Dordrecht.
- Main-Knorn, M., Pflug, B., Louis, J., Debaecker, V., Müller-Wilm, U., Gascon, F., 2017. Sen2Cor for Sentinel-2, in: Bruzzone, L., Bovolo, F., Benediktsson, J.A. (Eds.), Image and Signal Processing for Remote Sensing, SPIE, Warsaw, Poland, p. 3. <https://doi.org/10.1117/12.2278218>.
- Martins, V., Barbosa, C., de Carvalho, L., Jorge, D., Lobo, F., Novo, E., 2017. Assessment of atmospheric correction methods for Sentinel-2 MSI images applied to amazon floodplain lakes. *Remote Sens.* 9, 322. <https://doi.org/10.3390/rs9040322>.
- Marujo, R.F.B., Fronza, J.G., Soares, A.R., Queiroz, G.R., Ferreira, K.R., 2021. Evaluating the impact of LaSRC and Sen2cor atmospheric correction algorithms on Landsat-8/OLI and Sentinel-2/MSI data over AERONET stations in Brazilian territory. *ISPRS Ann. Photogramm. Remote Sens. Spatial Inf. Sci.* V-3–2021, 271–277. <https://doi.org/10.5194/isprs-annals-V-3-2021-271-2021>.
- Marzaietti, F., Cascone, S., Frate, L., Di Febraro, M., Acosta, A.T.R., Carranza, M.L., 2021. Measuring alpha and beta diversity by field and remote-sensing data: a challenge for coastal dunes biodiversity monitoring. *Remote Sensing* 13, 1928. <https://doi.org/10.3390/rs13101928>.
- McCarthy, B.C., Magurran, A.E., 2004. Measuring biological diversity. *J. Torrey Bot. Soc.* 131 (3), 277. <https://doi.org/10.2307/4126959>.
- Misra, G., Cawkwell, F., Winkler, A., 2020. Status of phenological research using Sentinel-2 data: a review. *Remote Sens.* 12, 2760. <https://doi.org/10.3390/rs12172760>.
- Moravec, D., Komárek, J., López-Cuervo Medina, S., Molina, I., 2021. Effect of atmospheric corrections on NDVI: Intercomparability of Landsat 8, Sentinel-2, and UAV Sensors. *Remote Sensing* 13, 3550. <https://doi.org/10.3390/rs13183550>.
- Onana, J.M., 2015. The World Flora Online 2020 project: will Cameroon come up to the expectation? *Rodriguésia* 66 (4), 961–972. <https://doi.org/10.1590/2175-7860201566403>.
- Onyia, N., Balzter, H., Berrio, J., 2019. Spectral diversity metrics for detecting oil pollution effects on biodiversity in the Niger Delta. *Remote Sensing* 11, 2662. <https://doi.org/10.3390/rs11222662>.
- Palmer, M.W., Earls, P.G., Hoagland, B.W., White, P.S., Wohlgenuth, T., 2002. Quantitative tools for perfecting species lists. *Environmetrics* 13 (2), 121–137. <https://doi.org/10.1002/env.516>.
- Peel, M.C., Finlayson, B.L., McMahon, T.A., 2007. Updated world map of the Köppen-Geiger climate classification.
- Pereira, H.M., Ferrier, S., Walters, M., Geller, G.N., Jongman, R.H.G., Scholes, R.J., Bruford, M.W., Brummitt, N., Butchart, S.H.M., Cardoso, A.C., Coops, N.C., Dulloo, E., Faith, D.P., Freyhof, J., Gregory, R.D., Heip, C., Hóft, R., Hurr, G., Jetz, W., Karp, D.S., McGeoch, M.A., Obura, D., Onoda, Y., Pettorelli, N., Reyers, B., Sayre, R., Scharlemann, J.P.W., Stuart, S.N., Turak, E., Walpole, M., Wegmann, M., 2013. *Essential Biodiversity Variables*. *Science* 339 (6117), 277–278.
- Pettorelli, N., Wegmann, M., Skidmore, A., Múcher, S., Dawson, T.P., Fernandez, M., Lucas, R., Schaepman, M.E., Wang, T., O'Connor, B., Jongman, R.H.G., Kempeneers, P., Sonnenschein, R., Leidner, A.K., Böhm, M., He, K.S., Nagendra, H., Dubois, G., Fatoyinbo, T., Hansen, M.C., Paganini, M., de Klerk, H.M., Asner, G.P., Kerr, J.T., Estes, A.B., Schmeller, D.S., Heiden, U., Rocchini, D., Pereira, H.M., Turak, E., Fernandez, N., Lausch, A., Cho, M.A., Alcaraz-Segura, D., McGeoch, M.A., Turner, W., Mueller, A., St-Louis, V., Penner, J., Vihervaara, P., Belward, A., Reyers, B., Geller, G.N., Boyd, D., 2016. Framing the concept of satellite remote sensing essential biodiversity variables: challenges and future directions. *Remote Sens Ecol Conserv* 2 (3), 122–131. <https://doi.org/10.1002/rse2.15>.
- Poilvé, H., 2010. *geoland2 - BioPar Methods Compendium of MERIS FR Biophysical Products*. <https://doi.org/10.13140/2.1.4205.1843>.
- Polley, H., Yang, C., Wilsey, B., Fay, P., 2019. Spectral heterogeneity predicts local-scale gamma and beta diversity of mesic grasslands. *Remote Sensing* 11 (4), 458. <https://doi.org/10.3390/rs11040458>.
- Portillo-Quintero, C., Hernández-Stefanoni, J.L., Reyes-Palomeque, G., Subedi, M.R., 2021. The road to operationalization of effective tropical forest monitoring systems. *Remote Sensing* 13, 1370. <https://doi.org/10.3390/rs13071370>.
- Randin, C.F., Ashcroft, M.B., Bolliger, J., Cavender-Bares, J., Coops, N.C., Dullinger, S., Dirnböck, T., Eckert, S., Ellis, E., Fernández, N., Giuliani, G., Guisan, A., Jetz, W., Joost, S., Karger, D., Lembrechts, J., Lenoir, J., Luoto, M., Morin, X., Price, B., Rocchini, D., Schaepman, M., Schmid, B., Verburg, P., Wilson, A., Woodcock, P., Yoccoz, N., Payne, D., 2020. Monitoring biodiversity in the Anthropocene using remote sensing in species distribution models. *Remote Sens. Environ.* 239, 111626. <https://doi.org/10.1016/j.rse.2019.111626>.
- Reddy, C.S., Kurian, A., Srivastava, G., Singhal, J., Varghese, A.O., Padalia, H., Ayyappan, N., Rajashekar, G., Jha, C.S., Rao, P.V.N., 2021. Remote sensing enabled essential biodiversity variables for biodiversity assessment and monitoring: technological advancement and potentials. *Biodivers Conserv* 30 (1), 1–14. <https://doi.org/10.1007/s10531-020-02073-8>.

- Rocchini, D., Marcantonio, M., Ricotta, C., 2017. Measuring Rao's Q diversity index from remote sensing: an open source solution. *Ecol. Ind.* 72, 234–238. <https://doi.org/10.1016/j.ecolind.2016.07.039>.
- Rocchini, D., Salvatori, N., Beierkuhnlein, C., Chiarucci, A., de Boissieu, F., Förster, M., Garzon-Lopez, C.X., Gillespie, T.W., Hauffe, H.C., He, K.S., Kleinschmit, B., Lenoir, J., Malavasi, M., Moudry, V., Nagendra, H., Payne, D., Šimová, P., Torresani, M., Wegmann, M., Féret, J.-B., 2021. From local spectral species to global spectral communities: a benchmark for ecosystem diversity estimate by remote sensing. *Ecol. Inf.* 61, 101195. <https://doi.org/10.1016/j.ecoinf.2020.101195>.
- Rouquié, B., Hagolle, O., Bréon, F.-M., Boucher, O., Desjardins, C., Rémy, S., 2017. Using Copernicus atmosphere monitoring service products to constrain the aerosol type in the atmospheric correction processor MAJA. *Remote Sensing* 9, 1230. <https://doi.org/10.3390/rs9121230>.
- Roy, D.P., Zhang, H.K., Ju, J., Gomez-Dans, J.L., Lewis, P.E., Schaaf, C.B., Sun, Q., Li, J., Huang, H., Kovalsky, V., 2016. A general method to normalize Landsat reflectance data to nadir BRDF adjusted reflectance. *Remote Sens. Environ.* 176, 255–271. <https://doi.org/10.1016/j.rse.2016.01.023>.
- Shi, T., Xu, H., 2019. Derivation of tasseled cap transformation coefficients for Sentinel-2 MSI at-sensor reflectance data. *IEEE J. Sel. Top. Appl. Earth Observ. Remote Sens.* 12 (10), 4038–4048. <https://doi.org/10.1109/JSTARS.2019.2938388>.
- Silva, F.B., Shimabukuro, Y.E., Aragão, L.E.O.C., Anderson, L.O., Pereira, G., Cardozo, F., Arai, E., 2013. Large-scale heterogeneity of Amazonian phenology revealed from 26-year long AVHRR/NDVI time-series. *Environ. Res. Lett.* 8 (2), 024011. <https://doi.org/10.1088/1748-9326/8/2/024011>.
- Skidmore, A.K., Pettorelli, N., Coops, N.C., Geller, G.N., Hansen, M., Lucas, R., Mûcher, C.A., O'Connor, B., Paganini, M., Pereira, H.M., Schaepman, M.E., Turner, W., Wang, T., Wegmann, M., 2015. Environmental science: agree on biodiversity metrics to track from space. *Nature* 523 (7561), 403–405. <https://doi.org/10.1038/523403a>.
- Sola, I., García-Martín, A., Sandoñis-Pozo, L., Álvarez-Mozos, J., Pérez-Cabello, F., González-Audicana, M., Montorio Llovería, R., 2018. Assessment of atmospheric correction methods for Sentinel-2 images in Mediterranean landscapes. *Int. J. Appl. Earth Obs. Geoinf.* 73, 63–76. <https://doi.org/10.1016/j.jag.2018.05.020>.
- Somvanshi, S.S., Kumari, M., 2020. Comparative analysis of different vegetation indices with respect to atmospheric particulate pollution using sentinel data. *Appl. Comput. Geosci.* 7, 100032. <https://doi.org/10.1016/j.acags.2020.100032>.
- Torresani, M., Rocchini, D., Sonnenschein, R., Zebisch, M., Marcantonio, M., Ricotta, C., Tonon, G., 2019. Estimating tree species diversity from space in an alpine conifer forest: The Rao's Q diversity index meets the spectral variation hypothesis. *Ecol. Inf.* 52, 26–34. <https://doi.org/10.1016/j.ecoinf.2019.04.001>.
- Tuomisto, H., Van doninck, J., Ruokolainen, K., Moulatlet, G.M., Figueiredo, F.O.G., Sirén, A., Cárdenas, G., Lehtonen, S., Zuquim, G., 2019. Discovering floristic and geoeological gradients across Amazonia. *J. Biogeogr.* 46 (8), 1734–1748. <https://doi.org/10.1111/jbi.13627>.
- Turney, C., Ausseil, A.-G., Broadhurst, L., 2020. Urgent need for an integrated policy framework for biodiversity loss and climate change. *Nat. Ecol. Evol.* 4, 996–996. <https://doi.org/10.1038/s41559-020-1242-2>.
- Vaglio Laurin, G., Puletti, N., Hawthorne, W., Liesenberg, V., Corona, P., Papale, D., Chen, Q., Valentini, R., 2016. Discrimination of tropical forest types, dominant species, and mapping of functional guilds by hyperspectral and simulated multispectral Sentinel-2 data. *Remote Sens. Environ.* 176, 163–176. <https://doi.org/10.1016/j.rse.2016.01.017>.
- Van Der Meer, F., Bakker, W., Scholte, K., Skidmore, A., De Jong, S., Clevers, J., Addink, E., Epema, G., 2001. Spatial scale variations in vegetation indices and above-ground biomass estimates: implications for MERIS. *Int. J. Remote Sens.* 22 (17), 3381–3396. <https://doi.org/10.1080/01431160152609227>.
- Vermote, E., Justice, C., Claverie, M., Franch, B., 2016. Preliminary analysis of the performance of the Landsat 8/OLI land surface reflectance product. *Remote Sens. Environ.* 185, 46–56. <https://doi.org/10.1016/j.rse.2016.04.008>.
- Vermote, E., Roger, J.C., Franch, B., Skakun, S., 2018. LaSRC (Land Surface Reflectance Code): Overview, application and validation using MODIS, VIIRS, LANDSAT and Sentinel 2 data's. In: IGARSS 2018–2018 IEEE International Geoscience and Remote Sensing Symposium. Presented at the IGARSS 2018–2018 IEEE International Geoscience and Remote Sensing Symposium, pp. 8173–8176. <https://doi.org/10.1109/IGARSS.2018.8517622>.
- Wang, R., Gamon, J.A., 2019. Remote sensing of terrestrial plant biodiversity. *Remote Sens. Environ.* 231, 111218. <https://doi.org/10.1016/j.rse.2019.111218>.
- Whittaker, R.H., 1972. Evolution and measurement of species diversity. *Taxon* 21 (2-3), 213–251. <https://doi.org/10.2307/1218190>.